Unusual Thermoelectric Behavior Indicating a Hopping to Bandlike Transport Transition in Pentacene

W. Chr. Germs, K. Guo, R. A. J. Janssen, and M. Kemerink*

Eindhoven University of Technology, PO Box 513 5600 MB Eindhoven, the Netherland

(Received 2 May 2012; published 6 July 2012)

An unusual increase in the Seebeck coefficient with increasing charge carrier density is observed in pentacene thin film transistors. This behavior is interpreted as being due to a transition from hopping transport in static localized states to bandlike transport, occurring at temperatures below ~250 K. Such a transition can be expected for organic materials in which both static energetic disorder and dynamic positional disorder are important. While clearly visible in the temperature and density dependent Seebeck coefficient, the transition hardly shows up in the charge carrier mobility.

DOI: 10.1103/PhysRevLett.109.016601 PACS numbers: 72.80.Le, 72.20.Pa

The increasing performance of organic semiconductors over the past decades has increased the technological interest in these materials, and vice versa. Considerable efforts notwithstanding, fundamental aspects of the charge transport in organic semiconductors are still the subject of debate. This holds, in particular, for the question to which extent the mobility, and its temperature and charge carrier density dependence, should be interpreted in terms of bandlike conduction. Because of energetic disorder, charge transport in organic semiconductors is often described within the framework of strong localization as developed by Anderson and Mott [1,2]. Anderson showed that in the presence of sufficiently strong static energetic disorder, localized tail states develop below a so-called mobility edge which separates them from delocalized states that are expected to dominate the charge carrier transport [1]. Later, Mott demonstrated that charge transport can also result from hopping processes between localized sites [2,3]. In organic semiconductors this picture is further complicated. Because of weak intermolecular bonding, thermally driven molecular vibrations give rise to significant dynamic disorder that limits the charge carrier mobility even in high-purity crystalline organic semiconductors where static disorder is minimized [4,5]. In these crystalline organic semiconductors these vibrations freeze-out at low temperature, giving rise to an increased mobility [6,7].

Polycrystalline and amorphous organic semiconductors behave differently. The increasing mobility with increasing temperature and charge density typically observed for these materials can be described in terms of either the mobility edge (ME) or multiple trapping and release model [8–10], or by the variable range hopping (VRH) model, [11–13]. The ME model implies bandlike conduction, the VRH model does not.

In this Letter we measure the Seebeck coefficient of polycrystalline pentacene in a thin film transistor (TFT) configuration. The Seebeck coefficient shows a remarkable increase with increasing charge carrier density, originating from a transition from hopping to bandlike conduction. The simultaneously measured charge carrier mobility increases with temperature and charge carrier density, but shows no noticeable signatures associated with the hopping to bandlike transport transition.

Several techniques can be used to investigate charge carrier transport in organic semiconductors [14]. Here we employ thermoelectric measurements which so far have hardly been applied to undoped organic semiconductors [15,16]. In particular, we measure the Seebeck coefficient of pentacene in a TFT configuration as a function of temperature and gate bias. By tuning the gate bias, we control the charge density and Fermi level E_F in pentacene. The Seebeck coefficient [17]

$$S = \frac{\int (E - E_F)\sigma(E)dE}{eT \int \sigma(E)dE}, \tag{1}$$

is determined by the difference between E_F and the energy E of the transporting states, i.e., the heat transported by the charge carriers. It therefore gives very direct insight in the energetics of the dominant charge transport processes. In (1), $\sigma(E)$ is the conductivity distribution function, T the temperature, and e the charge of the carrier. For bandlike transport within the ME model, where the current is carried by charges that are thermally excited over the mobility edge at energy E_C as illustrated in Fig. 1(a), Eq. (1) reduces to [17]:

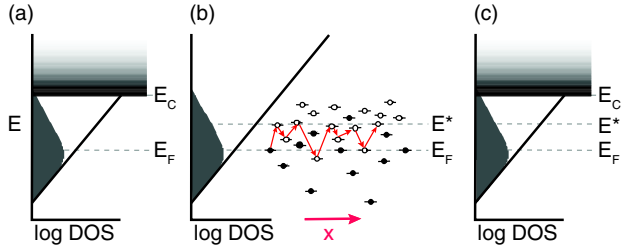

FIG. 1 (color online). The density of states used in (a) the ME model, (b) the VRH model, and (c) the hybrid model, including the relevant energy levels. The gray area below E_C represents the density of occupied localized states.

$$S_{\mathrm{ME}} = \frac{(E_{\mathrm{C}} - E_{\mathrm{F}})}{eT} + A, \tag{2}$$

with

$$A = \int_0^\infty \frac{\varepsilon}{eT}\sigma(\varepsilon)d\varepsilon \Big/ \int_0^\infty \sigma(\varepsilon)d\varepsilon,$$

where $\varepsilon = E - E_{\mathrm{C}}$.

In (2), the second term on the right-hand side accounts for excitations beyond the band edge and is typically 1%–20% of S_{ME}. Similarly, within the VRH model, where the transport is assumed to be dominated by a characteristic hop from the equilibrium energy to a relatively narrow transport energy E^* [18] as illustrated in Fig. 1(b), Eq. (1) becomes

$$S_{\mathrm{VRH}} = \frac{(E^* - E_{\mathrm{F}})}{eT}. \tag{3}$$

The usual behavior for the Seebeck coefficient is to decrease with increasing charge carrier density [19]. For bandlike transport, Eq. (2), this is explained by the Fermi level shifting towards the band edge. Likewise, for hopping transport, Eq. (3), E_{F} also shifts upward. Concomitantly, the number of unoccupied states near the Fermi level increases and consequently the transport energy E^* comes to lay closer to the Fermi level. To test this experimentally, we measured the Seebeck coefficient of pentacene in a TFT.

TFTs were built on a p^+-Si wafer, used as a gate, with 100 nm of thermally grown SiO_2 and an additional spin coated layer of 130 nm Cytop (an amorphous fluoropolymer available from Asahi Glass Company) as gate dielectric. The pentacene layer was deposited by thermal evaporation at 0.4 Å/s in a high vacuum system. Au source and drain top contacts are subsequently thermally deposited through a shadow mask to define the ~80 μm long and ~8 mm wide channel. Electrical characterization and Seebeck measurements were performed in a high vacuum probe station. The Seebeck coefficient at given temperature and gate bias was determined by linear fitting of the thermovoltage to $\Delta V = S\Delta T$, where the temperature difference ΔT across the channel of the TFT is generated by two Peltier elements.

By bringing the gate bias V_g to more negative potential, the charge density in the pentacene TFT is increased and Fig. 2 shows that at room temperature this indeed results in the expected decrease of S. Similar behavior was previously observed by Pernstich *et al.* and interpreted in terms of a ME model [15]. The room temperature behavior of S, i.e., to decrease with increasing hole density, is consistent with transport that is dominated by static energetic disorder. As explained above, depending on the model used, the decrease is explained by the shift of E_{F} to either the band edge E_{C} or the transport level E^*. The (positive) sign of S is consistent with p-type transport.

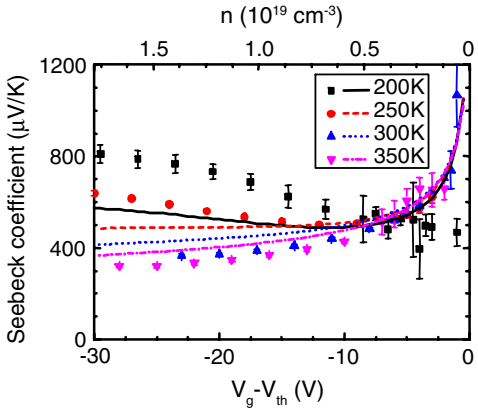

FIG. 2 (color online). Measurements (symbols) and calculations (lines) of the Seebeck coefficient vs gate bias in a pentacene thin film transistor. The gate bias V_g is corrected for the threshold voltage V_{th} of the TFT.

Surprisingly, when decreasing the temperature to below room temperature, we see an increase of S with increasing charge carrier density at $T = 250$ K and even more pronounced at $T = 200$ K. Clearly, such an increase in S cannot be explained using VRH or ME alone, as both predict a strictly monotonously decreasing density dependence.

Enhancement of the Seebeck coefficient at lower temperatures could in principle be due to phonon drag effects which are typically observable below roughly a quarter of the Debye temperature T_D [20]. Since T_D is in the range 125–216 K in pentacene [21,22], the onset of possible phonon drag effects is expected at far lower temperatures than observed.

To explain the increase of S with charge carrier density we developed a simplified hybrid model that incorporates both VRH and ME transport. It accounts for the contributions to the charge and energy transport by two processes that are treated as independent: VRH-type processes that occur within an exponential tail of localized states and transport by charges that are thermally excited to bandlike states above a mobility edge. For this model the density of states (DOS) and transport parameters are determined by fitting to the temperature dependent field-effect mobility measured on the same sample (Fig. 3).

As indicated in Fig. 1(c) the DOS is simplified to a single exponential trap tail below the mobility edge and a constant density of extended states above E_{C},

$$G(E) = \begin{cases} \frac{n_{\mathrm{trap}}}{k_{\mathrm{B}}T_0}\exp\left(-\frac{E}{k_{\mathrm{B}}T_0}\right) & \text{for } E < E_{\mathrm{C}}, \\ \frac{n_0}{k_{\mathrm{B}}T_0} & \text{for } E \geq E_{\mathrm{C}}, \end{cases} \quad (E_{\mathrm{C}} = 0), \tag{4}$$

where n_0 is divided by $k_{\mathrm{B}}T_0$ for dimensional reasons. The number of charge carriers above E_{C}, n_{free}, follows from the Fermi-Dirac distribution. The exact shape of the DOS above E_{C} can have some influence on the charge transport;

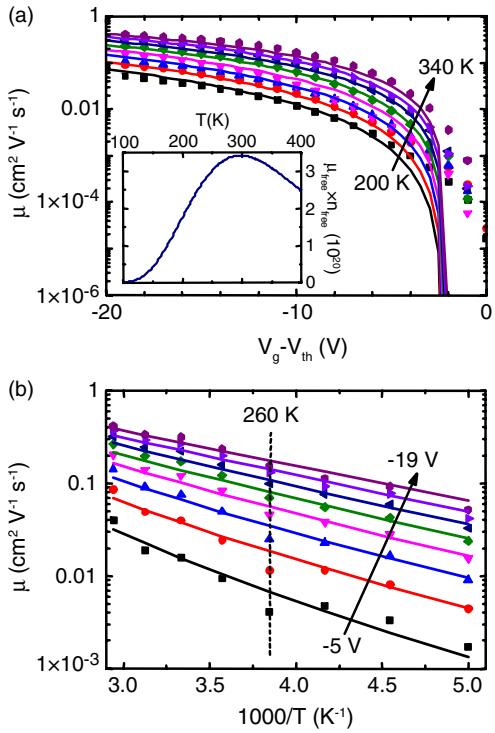

FIG. 3 (color online). (a) The measured (symbols) and calculated (lines) linear mobility vs gate bias with intervals of $T = 20$ K. The deviations at small gate voltage are attributed to leakage currents and the breakdown of the assumption that $|V_g - V_{\text{th}}| \gg V_{\text{sd}}$ (V_{sd} = source-drain voltage). The inset shows $\mu_{\text{free}} \cdot n_{\text{free}} (\sim \sigma_{\text{ME}})$ vs T for $V_g - V_{\text{th}} = -30$ V. (b) Activation plot of the measured (symbols) and calculated (lines) mobility for different gate bias, with intervals of 2 V

however the small contribution of the second term A in Eq. (2) shows that this is usually of relatively minor importance. The conductivity in the ME part of the model is calculated as $\sigma_{\text{ME}} = e n_{\text{free}} \mu_{\text{free}}(T)$, with μ_{free} the band mobility. In order to account for the inherently large thermal lattice fluctuations in molecular semiconductors we assume μ_{free} to follow a power law dependence on temperature: [4,5,7]

$$\mu_{\text{free}}(T) = \mu_0 T^{-m}. \tag{5}$$

The VRH part is described by the Mott-Martens model that assumes transport to be dominated by hops from the Fermi level to the transport level E^* [11,23]. The position of this level and the typical hopping distance R^* are connected via a percolation argument [11,20]

$$B_{\text{C}} = \frac{4}{3} \pi R^{*3} \int_{E_{\text{F}}}^{E^*} G(E) dE, \tag{6}$$

with $B_{\text{C}} = 2.8$ the critical number of bonds. The conductivity is subsequently calculated by optimizing a Miller-Abrahams-type expression $\sigma_{\text{VRH}} = \sigma_0 \exp[-2\alpha R^* - (E^* - E_F)/(k_{\text{B}} T)]$ [3,20], with α the inverse localization length, k_{B} the Boltzmann constant, and σ_0 the conductivity prefactor. This implementation of the VRH part is essentially identical to that of Ref. [13]. The total conductivity of the hybrid model is simply the sum of the ME and VRH contributions, viz., $\sigma_{\text{hyb}} = \sigma_{\text{ME}} + \sigma_{\text{VRH}}$. Consistent with Eq. (1), the Seebeck coefficient of the hybrid model is calculated as the conductivity-weighted average of the two contributing transport channels:

$$S = \frac{S_{\text{ME}} \sigma_{\text{ME}} + S_{\text{VRH}} \sigma_{\text{VRH}}}{\sigma_{\text{ME}} + \sigma_{\text{VRH}}}. \tag{7}$$

The mobility measurements and the fitting results are shown in Fig. 3; the used parameters are given in Table I. No distinctive features are visible. The mobility increases with increasing (negative) gate bias and decreases with decreasing temperature. Both are consistent with earlier observations for polycrystalline pentacene [12] and suggest (static) energetic disorder dominated transport over the entire measurement range. Unsurprisingly, bare VRH and ME models give rather accurate fits to the mobility data (see Supplemental Material Figs. S3-S6 [24]). The somewhat better fit quality of the hybrid model could, in the case of the mobility data, also be attributed to the larger number of free parameters.

In Fig. 3(b), the measured mobility might seem to show a slightly different activation behavior above and below 260 K, which is around the transition temperature in the Seebeck behavior, but the effect is too small to make definitive statements. The calculated curves in Fig. 3(b) do show a slight bend which is due to the changing ratio of $\sigma_{\text{VRH}}/\sigma_{\text{ME}}$. The corresponding Seebeck coefficients are shown as lines in Fig. 2. Although the agreement with experiment is only qualitative, the characteristic features are well reproduced. In particular, the 200 K curve reproduces the unusual increase in the Seebeck coefficient curve beyond a gate bias of -10 V. The increase is explained by a shift from entirely hopping-dominated conduction at low gate bias to conduction in which bandlike states above the mobility edge play an important role. This is illustrated in Fig. 4.

At 200 K the heat transported at the mobility edge ($E_{\text{C}} - E_F$) and the heat transported at the transport level ($E^* - E_{\text{F}}$) both decrease with increasing charge carrier

TABLE I. Parameters used in the calculations with the hybrid model.

n_{trap}	10^{26} m^{-3}
T_0	1000 K
σ_0	2.3×10^6 S m^{-1}
a^{-1}	9 Å
$\mu_0 n_0$[a]	5.3×10^{38} m^{-1} V^{-1} s^{-1}
m	-6

[a]The mobility prefactor μ_0, and density of bandlike states above the mobility edge, n_0, are fitted as the product of the two because of their interdependence.

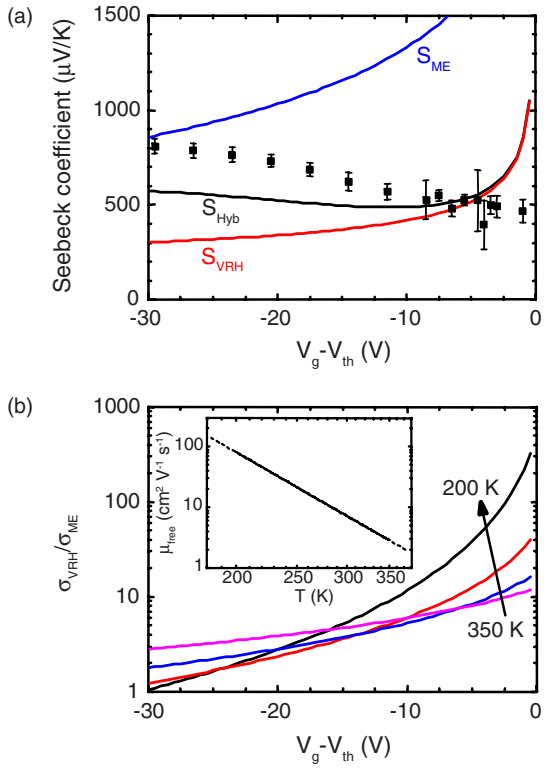

FIG. 4 (color online). (a) Measured (symbols) and calculated (lines) Seebeck coefficients at $T = 200$ K. S_{hyb} is the conductivity-weighted average of S_{VRH} and S_{ME}. (b) The ratio of the VRH and the ME contributions to the conductivity vs gate bias for different temperatures. The inset shows the temperature dependent band mobility μ_{free} assuming $n_0 = 10^{27}$ m^{-3} for the DOS above E_C.

density, accounting for the downward trends in S_{ME} and S_{VRH} in Fig. 4(a). With increasing density the Fermi level moves towards the band edge. Since E^* does, and E_C does not shift up with E_F, the relative contribution from hopping conduction goes down, as is shown by the ratio σ_{VRH}/σ_{ME} in Fig. 4(b). Consequently, the weight-averaged Seebeck coefficient S_{hyb} shifts from the S_{VRH} curve at small gate bias up towards S_{ME} for large gate bias. The relatively large value of S_{ME} at lower temperatures follows from Eq. (2) and the temperature independence of E_C. In contrast, E^* decreases with T, making S_{VRH}, Eq. (3), relatively temperature independent (see also Figs. S1 and S2 in [24]).

A remarkable consequence of these observations is that in the investigated temperature window, and at higher charge densities ($V_g - V_{th} < -20$ V), the contribution of VRH to the total conductivity actually *decreases* with decreasing temperature. The opposite would be expected from VRH hopping theory when applied to an energetically disordered inorganic semiconductor [3]. In the present system, due to the freezing-out of molecular vibrations in the pentacene, the band mobility μ_{free} increases strongly at lower T, shifting the balance in the charge transport to bandlike conduction despite the increasing energetic penalty for thermal activation over the mobility edge. The temperature dependence of the band mobility, $\mu_{free}(T) = \mu_0 T^{-6}$ that is plotted in the inset of Fig. 4(b) is, for the presently probed temperature window, not unrealistic in view of the calculations by Ortmann *et al.* [25] It is, however, rather strong in comparison to experimental observations on p- and n-type single crystal devices [26–30]. However, in the latter case typically the effective mobility is probed, which can be substantially below the free mobility due to the fact that only a fraction of the carriers contributes to the actual transport [7,28,29]. We have therefore plotted the product $\mu_{free} \cdot n_{free}$ in the inset to Fig. 3(a). Interestingly, the curve first shows an increase in mobility followed by a (stronger) decrease with decreasing temperature. Such behavior has been observed on a number of single crystal organic field-effect transistor devices [26,27,29,30] and was actually interpreted in terms of a ME model that is similar to what is used here [29,30]. More details can be found in Figs. S7 and S8 of the Supplemental Material [24].

Summarizing, we have shown that at lower temperatures the Seebeck coefficient in a pentacene thin film transistor displays an unusual increase with increasing gate bias. The increase is explained by a transition from variable range hopping-dominated transport at low gate bias to more pronounced bandlike transport at high gate bias. A simplified hybrid model that accounts for both types of charge transport gives a qualitative description of the observed thermoelectric behavior. These findings confirm that charge transport in polycrystalline organic semiconductors can simultaneously be affected by two types of disorder: static energetic disorder resulting from, e.g., charges in the gate dielectric [31,32], and dynamic positional disorder driven by molecular vibrations. Finally, the temperature and density dependence of the simultaneously measured charge carrier mobility shows no notable features, making it hard, if not impossible, to distinguish transport models on the basis of such data alone.

This research is supported by the Dutch Technology Foundation STW, which is the applied science division of NWO, and the Technology Programme of the Ministry of Economic Affairs (VIDI Grant No. 07575).

*Corresponding author.
m.kemerink@tue.nl

[1] P. W. Anderson, Phys. Rev. **109**, 1492 (1958).
[2] N. F. Mott, J. Phys. C **20**, 3075 (1987).
[3] N. F. Mott and E. A. Davis, *Electronic Processes in Non-Crystalline Materials* (Oxford University Press, Oxford, England, 1979), 2nd ed..
[4] A. Troisi and G. Orlandi, Phys. Rev. Lett. **96**, 086601 (2006).
[5] S. Fratini and S. Ciuchi, Phys. Rev. Lett. **103**, 266601 (2009).
[6] T. Sakanoue and H. Sirringhaus, Nature Mater. **9**, 736 (2010).

[7] M. E. Gershenson, V. Podzorov, and A. F. Morpurgo, Rev. Mod. Phys. **78**, 973 (2006).
[8] G. Horowitz, R. Hajlaoui, and P. Delannoy, J. Phys. III **5**, 355 (1995).
[9] A. R. Völkel, R. A. Street, and D. Knipp, Phys. Rev. B **66**, 195336 (2002).
[10] A. Salleo, T. W. Chen, A. R. Völkel, Y. Wu, P. Liu, B. S. Ong, and R. A. Street, Phys. Rev. B **70**, 115311 (2004).
[11] R. Coehoorn, W. F. Pasveer, P. A. Bobbert, and M. A. J. Michels, Phys. Rev. B **72**, 155206 (2005).
[12] M. C. J. M. Vissenberg and M. Matters, Phys. Rev. B **57**, 12964 (1998).
[13] W. S. C. Roelofs, S. G. J. Mathijssen, R. A. J. Janssen, D. M. de Leeuw, and M. Kemerink, Phys. Rev. B **85**, 085202 (2012).
[14] N. Karl, Synth. Met. **133–134**, 649 (2003).
[15] K. P. Pernstich, B. Rossner, and B. Batlogg, Nature Mater. **7**, 321 (2008).
[16] A. von Mühlenen, N. Errien, M Schaer, M.-N. Bussac, and L. Zuppiroli, Phys. Rev. B **75**, 115338 (2007).
[17] H. Fritzsche, Solid State Commun. **9**, 1813 (1971).
[18] S. D. Baranovskii, T. Faber, F. Hensel, and P. Thomas, J. Phys. Condens. Matter **9**, 2699 (1997).
[19] A. Shakouri, Annu. Rev. Mater. Res. **41**, 399 (2011).
[20] A. B. Kaiser, S. A. Rogers, and Y. W. Park, Mol. Cryst. Liq. Cryst. **415**, 115 (2004).
[21] M. Fulem, V. Lastovka, M. Straka, K. Ruzicka, and J. M. Shaw, J. Chem. Eng. Data **53**, 2175 (2008).
[22] R. C. Hatch, D. L. Huber, and H. Höchst, Phys. Rev. Lett. **104**, 047601 (2010).
[23] H. C. F. Martens, I. N. Hulea, I. Romijn, H. B. Brom, W. F. Pasveer, and M. A. J. Michels, Phys. Rev. B **67**, 121203 (2003).
[24] See Supplemental Material at http://link.aps.org/supplemental/10.1103/PhysRevLett.109.016601 for 'separate VRH- and ME-contributions to S from the hybrid model, an analysis of the experimental data with a purely VRH- or ME-model, and the effective conductivity for the ME contribution to the hybrid model.
[25] F. Ortmann, F. Bechstedt, and K. Hannewald, Phys. Rev. B **79**, 235206 (2009).
[26] V. Podzorov, E. Menard, A. Borissov, V. Kiryukhin, J. A. Rogers, and M. E. Gershenson, Phys. Rev. Lett. **93**, 086602 (2004).
[27] O. D. Jurchescu, J. Baas, and T. T. M. Palstra, Appl. Phys. Lett. **87**, 052102 (2005).
[28] V. Podzorov, E. Menard, J. A. Rogers, and M. E. Gershenson, Phys. Rev. Lett. **95**, 226601 (2005).
[29] H. Xie, H. Alves, and A. F. Morpurgo, Phys. Rev. B **80**, 245305 (2009).
[30] N. A. Minder, S. Ono, Z. Chen, A. Facchetti, and A. F. Morpurgo, Adv. Mater. **24**, 503 (2012).
[31] J. Veres, S. Ogier, G. Lloyd, and D. de Leeuw, Chem. Mater. **16**, 4543 (2004).
[32] A. Sharma, N. M. A. Janssen, S. G J. Mathijssen, D. M. de Leeuw, M. Kemerink, and P. A. Bobbert, Phys. Rev. B **83**, 125310 (2011).